SINTECHCOM: Science, Technology and Communication Journal
Vol. 4, No. 2, February 2024, pp. 51-62, DOI: 10.59190/stc.v4i2.260

Peatland aquifer zone modeling via Wenner and Schlumberger configuration geoelectric strategies in Tarai Bangun Village, Riau Province, Indonesia

Tumbur Marudut Tua Sitinjak, Juandi Muhammad*, Rahmi Dewi
Department of Physics, Universitas Riau, Pekanbaru 28293, Indonesia

ABSTRACT

The quality of freshwater in peatland areas poses significant concerns for both governmental bodies and local communities. Challenges arise during well drilling activities, where individuals often encounter difficulties in accessing fresh water, either due to its absence or contamination with peat-infused water. Tarai Bangun Village, situated in the Kampar Regency of Riau, represents a critical peatland region warranting thorough investigation, particularly along street of Sarana Utama. Despite lacking social amenities such as markets, the area is equipped with essential facilities like schools and places of worship. This study aims to assess the efficacy of Wenner and Schlumberger configuration modeling in horizontal and vertical soil mapping, thereby facilitating a comprehensive understanding of groundwater distribution and aquifer zoning within the peatland areas under examination. Analysis conducted utilizing Res2DInv software for horizontal modeling revealed significant findings. In track 1, groundwater layers were identified at depths of 6.50 meters and 19 meters, comprising gravel, sandstone, and limestone. Track 2 exhibited an aquifer layer spanning depths from 2.50 meters to 24.9 meters, consisting of alluvium, gravel, and limestone. Furthermore, interpretation of 1D geoelectric vertical model cross-sections using Progress software unveiled additional insights. Path 1 delineated depths of 0.12 meters, 19.30 meters, and beyond 41.28 meters, featuring a lithological composition of sandstone, limestone, and dry gravel. Path 2 showcased depths of 0.14 meters, 9.43 meters, and exceeding 12.02 meters, characterized by dry sand and gravel formations.

ARTICLE INFO

Article history:

Received Nov 10, 2023
Revised Jan 16, 2024
Accepted Feb 19, 2024

Keywords:

Aquifer
Geoelectric
Peatland
Schlumberger
Wenner

* **Corresponding Author**
E-mail address: juandi@lecturer.unri.ac.id

1. INTRODUCTION

Peatlands are a collection of organic matter that has decomposed over thousands of years in watery conditions [1, 2]. The low water quality in peatlands can lead to unhealthy environments because peat water has a low pH and a high level of heavy metal content. Indonesia has 17.2 million hectares of peatland spread across various islands such as Sumatra, Kalimantan, and Papua. Sumatra Island has 6.4 million hectares (43% of Indonesia's peatland) with 56.6% located in Riau Province [3-5]. Peatlands have the capacity to absorb water up to 13 times their weight, thus playing a role in reducing flood risk and potentially containing high levels of organic matter [6, 7]. Peatlands also have characteristics such as low bulk density, high porosity, and high acidity levels. According to Soewandita (2018), about 85% – 95% of the water content in peatlands is undrained, so even though the top layer may be dry, the lower area of the peatland remains moist [8]. The presence of water in peatlands functions as a source of fresh water in significant volumes, reaching 8 – 13 times the volume of the peat itself. The potential that needs to be managed in peatlands concerns fresh water.

Freshwater is water that is safe for human consumption, making up about 2.5% of the total water composition on Earth. Freshwater sources can be found in lakes, rivers, snow, or well water, which represents one of the groundwater variants utilized to support the life of humans, animals, and plants. In areas inefficient at absorbing water, there is direct runoff from the ground surface to rivers, lakes, and seas without the process of absorption into the ground. This condition causes a limitation of water supply [9-11]. The scarcity of freshwater on Earth poses a challenge that needs to be overcome, and the search for groundwater sources by identifying lithology or the types of rocks capable of storing aquifers potentially becomes productive aquifers, thus meeting the needs for clean water [12, 13]. An aquifer is a permeable underground layer that contains water along with rocks, fissures, and unconsolidated materials. Geoelectric measurements aim to investigate physical concepts in the Earth's layers, including the method of specific resistance of the subsurface. This is done to identify the distribution of specific resistance in aquifers that form the subsurface layer, and to interpret data from the measurements obtained [14-16]. One way to do this is by using geoelectric methods. Geoelectric methods are among the geophysical methods that are easy, efficient, and produce data with a wide range. Several researchers have conducted studies on groundwater aquifer layers using the Wenner Configuration and Schlumberger Configuration geoelectric methods.

The geoelectric method uses 4 electrodes, where 2 are current electrodes and 2 are potential electrodes. The principle of this method uses the concept of electric current propagation in the Earth's heterogeneous medium, with the ratio between the measured potential difference and the magnitude of the electric current injection reflecting the resistivity values of various media beneath the Earth's surface. By conducting a resistivity analysis between different media or types of rocks, accurate results can be obtained. Geoelectric data interpretation is crucial in depicting the subsurface image. Each rock layer has its resistivity value and characteristics [17-19]. Based on the research regarding the determination of aquifer layers using the Wenner configuration geoelectric method in the Bumi Kualu Damai III Housing area, Tarai Bangun Village, Tambang District, Kampar Regency, the results stated that based on its resistivity values, the aquifer layer in the study area is located at a depth of up to 19.8 meters below the ground surface with resistivity values ranging from 52.9 – 593 Ωm. The subsurface lithology in this study area is a peat layer with resistivity values of 84.6 – 195 Ωm. The water quality is not yet suitable for consumption due to its highly acidic nature, but it is still safe and suitable for other needs such as washing, bathing, and more. The issue of clean water quality in peatland areas has become a concern for both the government and the community. Challenges are encountered in the field when residents attempt to drill wells, only to find no freshwater or to discover it contaminated with peat water. Tarai Bangun Village, Kampar Regency, one of the areas in Riau that is situated on peatland, requires attention for study, particularly on street of Sarana Utama. Around the location of this study, there are no social facilities used by residents such as markets. However, other social facilities are available, including schools and places of worship. The use of Wenner and Schlumberger configuration modeling is expected to be a step in mapping the soil horizontally and vertically, thus providing a cross-section of groundwater distribution and aquifer zoning in the peatland area of the study site. Given the background outlined above, the research question raised in this study is what the condition of the aquifer distribution pattern is in the peatlands of Tarai Bangun Village, Tambang District. Considering the study location area still faces significant clean water issues, as residents attempting to drill wells either fail to find freshwater or find it contaminated with peat water. Thus, to this day, in the research location, there are only a few residential areas occupied by the community.

2. RESEARCH METHODS

2.1. Research Location

This study was conducted in Tarai Bangun Village, Kampar Regency, Riau, utilizing the Schlumberger and Wenner geoelectric configuration methods to analyze primary data collected from the field. These geoelectric methods were used to identify aquifers by varying the subsurface resistivity values. The geographical location of the study can be seen in Figure 1. This research used two tracks, each 300 meters in length, for data collection at the research site. The first track is marked with an orange line symbol at the coordinates 0°25'16.2"N 101°19'50.1"E. Meanwhile, the second track is marked with a red line symbol and has the coordinates 0°25'20.8"N 101°19'50.3"E.

Figure 1. Research location map.

2.2. Research Equipment Preparation

After determining the length of the track to be used, the starting point of the track is set as the starting point for measurements, and the coordinates of this point can be identified using a GPS. Then, the spacing distance (a) between potential electrodes (P_1P_2) and current electrodes (C_1C_2) is set at 5 meters each, and both electrodes are inserted into the ground. Once the electrodes are in place, the winding cable is connected to the current electrodes (C_1C_2) and the potential electrodes (P_1P_2) to link the electrodes with the resistivity meter, which serves as a conduit for current and potential. Next, the resistivity meter is connected to a car battery, and connector cables are used to connect the battery to the (+) and (-) input jacks on the resistivity meter. The equipment used for data retrieval can be seen in Appendix 3 of the research materials.

2.3. Measurement and Data Collection using a Resistivity Meter

The resistivity meter is turned on by pressing the power button from the off to on position. When the current loop indicator points to the right, the resistivity meter is considered ready for use. If not, the connection needs to be adjusted by deepening the current electrodes. Next, the resistivity meter button is pressed until the voltage display (V) approaches zero or shows a zero reading. The start button is then pressed to inject current until the current display (mA) shows a stable data reading. Lastly, the hold button is pressed to facilitate reading the current on the display as well as the potential, and the measurement data that appears is recorded. The study is conducted by moving each electrode according to the rules of the Schlumberger and Wenner configurations until the end of the track. Measurements are taken several times by setting a number of tracks between electrodes.

2.4. Data Processing with Microsoft Excel

The data collected from the research, consisting of current values and potential differences, are further processed using the Microsoft Excel application to generate geometric factor values, apparent resistivity, and datum points.

2.5. Data Interpretation with Progress and Res2DInv Software

In this study, the obtained data are processed using Progress Software for the Schlumberger configuration and Res2DInv Software for the Wenner configuration. These software programs are used to determine the true resistivity values from the previously calculated apparent resistivity data

using Microsoft Excel. To accomplish this, an inversion model is created based on the calculations of the apparent resistivity data. The result of this process is interpretation in the form of one-dimensional (1D) profiles for the Schlumberger configuration and two-dimensional (2D) profiles for the Wenner configuration, depicting the subsurface structure of the research site. To ensure accurate resistivity interpretation, geological data from the research area is required as support. This geological data helps strengthen the resistivity values of the subsurface media produced through Progress and Res2DInv software. Thus, this study combines resistivity information from Progress and Res2DInv software with geological data to better understand the subsurface characteristics at the research site.

2.6. Data Analysis

The subsurface imagery generated by Progress Software consists of line graphs based on geoelectric interpretation supported by a table relating resistivity values to rock types. Meanwhile, the subsurface imagery produced by Res2DInv Software is a colored representation containing information about resistivity values beneath the ground, which can assist in identifying lithological arrangements beneath the surface as well as the depth of rocks. This is done by referring to the range of resistivity values classified, while also considering regional geological data from the research area. Thus, determining the subsurface layers in hot spring areas can be done more accurately.

2.7. Procedure for Geoelectric Data Processing

The procedure for processing geoelectric data can be outlined as follows:

2.7.1. Processing Geoelectric Data with Progress Software

The measurement results obtained from the research site in the form of resistivity data are processed using Progress software. The resistivity data is first calculated, and then the geometric factor values are calculated using an Equation. The steps for using Progress software to process geoelectric data are as follows:

1. Measurement data consisting of current electrode AB values, potential electrode MN values, current strength I, and voltage V are processed using Microsoft Excel to determine the geometric factor and apparent resistivity values.
2. The processed data from Microsoft Excel is then copied into Notepad and inputted into the Progress software by entering the AB/2 value and the apparent resistivity value.
3. After inputting the values, the processed data results in a graph displaying resistivity values and lithology for each layer, along with thickness values.
4. The obtained graph and mapping can be used to model resistivity by matching lithology with corresponding resistivity values and depths.

2.7.2. Processing Geoelectric Data with Res2DInv Software

Once the data is obtained, data processing is performed. Data processing for resistivity geoelectric data uses Res2DInv software. Res2DInv software automatically determines a two-dimensional (2D) resistivity model to determine the subsurface from resistivity geoelectric survey data. The data processing process with the steps performed is as follows:

1. The data obtained from the measurement results, including electrode spacing length, injected current (I), and potential difference (V) generated from observation points, is processed using Microsoft Excel to calculate geometric factors and resistivity values.
2. The calculated data is then copied to Notepad, and inputted into the Progress software to produce processed data in the form of a graph displaying resistivity values for each layer along with depth values from the generated data.
3. Apparent resistivity values are calculated from the measurement configuration factors and the comparison of potential difference (ΔV) and current strength (I) measurements.

3. RESULTS AND DISCUSSIONS

Field data collection was carried out using the Wenner configuration method or horizontal model, where two tracks were made with each track measuring 300 meters in length. The modeling results of the Wenner configuration are represented by different colors variations on the vertical axis, indicating depth in meters, while the horizontal axis depicts the electrode positions in meters.

3.1. Interpretation of Horizontal Geoelectric Data – Track 1

Track 1 is located at coordinates 0°25'10.0"N 101°19'46.9"E and extends from north to east. The modeling results of track 1 using the Res2DInv software can be seen in Figure 1.

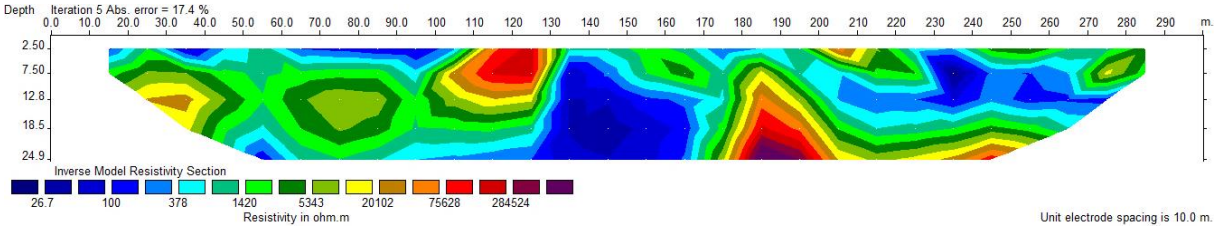

Figure 2. Subsurface resistivity model of track 1 using Res2DInv.

According to Choudhury et al. (2001) [20], there are various variations in resistivity values in the subsurface layers. The difference in resistivity values between peat and other substrates can be used as an indicator to identify underground structures. Figure 2 illustrates various types of layers with specific resistivity values indicating the composition of materials within them. An aquifer layer is a geological formation that can store and transmit water underground, with the ability to move water in sufficient quantities to support economic development [21]. An aquifer can also be interpreted as a layer that allows water to be stored and flow, or what is called a permeable layer, such as sand or gravel. Conversely, a layer that cannot be penetrated by groundwater is called an impermeable layer, such as a clay layer. In track 1, the lowest resistivity value is 26.7 Ωm and the highest resistivity value reaches 284,524 Ωm. This highest resistivity value indicates a depth of subsurface layers of up to 24.9 meters, resulting in measurement accuracy with an RMS-error of 17.4%. The interpretation results of resistivity value measurements on track 1 can be seen in Table 1.

Table 1. Description of interpretation results - track 1 Wenner configuration.

Resistivity (Ωm)	Depth (m)	Distance (m)	Rock type	Information
26.7 – 100	2.50 – 24.9	30 – 45 65 – 100 135 – 160 230 – 280	Clay and sand	Non aquifer
100 – 378	2.50 – 24.9	15 – 280	Some clay and gravel	Aquifer
378 – 5,343	6.50 – 24.9	15 – 130 130 – 175 175 – 285	Gravel and sandstone	Aquifer
5,343 – 20,102	2.5 - 19	15 – 50 60 – 90 155 – 165 175 – 285	Limestone	Aquifer
75,628 – 284,524	12.8 – 24.9	115 – 125 180 – 200	Quartzite	Non aquifer

The first layer, which has resistivity values ranging from 26.7 – 100 Ωm, is located at depths ranging from 2.50 – 24.9 meters. This layer can be identified by its dark blue color and interpreted as a medium peat layer containing a mixture of clay and sand. The second layer is characterized by variations in color from dark blue to light blue and has resistivity values of 100 – 378 Ωm, also found at the same depths ranging from 2.50 – 24.9 meters. This layer likely consists of some clay and gravel. The third layer has resistivity values ranging from 378 – 5,343 Ωm and is marked by light green to dark green colors. It is spread from depths of 6.50 – 24.9 meters and can be interpreted as dry gravel and sandstone. The fourth layer, ranging in color from dark green to light brown, has resistivity values of 5,343 – 20,102 Ωm. This layer is located at depths of 2.5 – 19 meters and identified as limestone. The last layer or the fifth layer, which spreads from depths of 12.8 – 24.9 meters, is quartzite rock with

resistivity values ranging from 75,628 – 284,524 Ωm. This layer is characterized by colors varying from orange to purple.

3.2. Interpretation of Horizontal Geoelectric Data – Track 2

Track 2 is located at coordinates 0°25'10.0"N 101°19'46.9"E. The modeling results of track 2 using the Res2DInv software are clearly depicted in Figure 3. The Res2DInv software is utilized to obtain a 2D geoelectric cross-sectional model consisting of layer depths and resistivity variations as a reference for interpreting the types of materials or rocks present beneath the earth's surface. In this model, it is evident that the lowest resistivity value is 1.49 Ωm, reaching up to a maximum resistivity of 77064 Ωm. Additionally, the interpretation results indicate that the depth below the surface along track 2 is 24.9 meters with an error value of 17.5%, covering a track length of 300 meters with measurement point spacing of 10 meters.

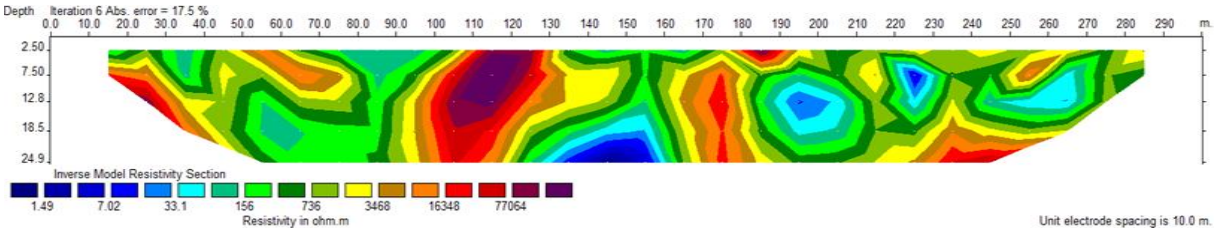

Figure 3. Subsurface resistivity model of track 2 using Res2DInv.

Figure 3 illustrates the 2D resistivity cross-section of track 2. The interpretation results of track 2 data reveal several layers identifiable based on resistivity values. The first layer, with resistivity values ranging from 1.49 – 33.1 Ωm, is situated at depths from 7.50 – 24.9 meters. This layer is characterized by dark blue to light blue colors in the image and interpreted as a shallow peat layer containing clay and sand. The second layer, interpreted as alluvial deposits and gravel, is indicated by variations in colors from light green to dark green with resistivity values ranging from 156 – 736 Ωm. This layer is located at depths from 2.5 – 24.9 meters. Meanwhile, the third layer, with resistivity values of 736 – 16,348 Ωm, is identified as limestone. This layer is marked by light green to orange colors in the image and is located at the same depths of 2.5 – 24.9 meters. The last layer, ranging in depth from 2.5 – 24.9 meters and shown with variations in colors from orange to purple with resistivity values ranging from 16,348 – 77,064 Ωm, is interpreted as quartzite. The interpretation results of track 2 data can be seen in Table 2.

Table 2. Description of track 2 interpretation results Wenner configuration.

Resistivity (Ωm)	Depth (m)	Distance (m)	Rock type	Information
1.49 – 33.1	7.50 – 24.9	130 – 160 190 – 205 220 – 230 250 – 265	Clay and sand	Non aquifer
156 – 736	2.5 – 24.9	15 – 285	Alluvium	aquifer
736 – 16,348	2.5 – 24.9	15 – 80 90 – 150 160 – 200 210 – 270	Limestone	aquifer
7706 – 16,348	2.5 – 24.9	100 – 130	Quartzite	Non aquifer

Field data collection was conducted using the Schlumberger configuration or horizontal model, where two tracks were carried out with each track having a length of 300 meters. The modeling results from the Schlumberger configuration are represented by the actual apparent resistivity values on the vertical axis, indicated in ohmmeters, while the horizontal axis depicts the electrode depth positions in meters.

3.3. Interpretation of Vertical Geoelectric Data Model – Track 1

Track 1 has a length of 300 meters with a spacing of 10 meters. This track is located at coordinates 0°25'10.0"N 101°19'46.9"E and runs from north to east. The modeling results of track 1 using the Progress software can be seen in Figure 4 below. From the model, it is observed that the resistivity values range from 21.99 – 3293.62 Ωm, and the interpretation results state that the depth below the surface along track 1 is 60.00 meters with an error value of 12.16%.

Figure 4 depicts the subsurface layer structure of the soil on track 1 with a total of 7 layers identifiable using the vertical model. The first layer, ranging from the surface to a depth of 0.12 meters, shows a resistivity value of 21.99 Ωm and is interpreted as a mixture of sand and clay. The second layer, with a depth of 0.12 – 6.08 meters and a resistivity value of 3293.62 Ωm, is interpreted as sandstone and limestone. Next, the third layer, located at depths from 6.08 – 19.30 meters, shows a resistivity value of 1864.05 Ωm and is identified as dry sandstone and gravel. The fourth layer, with a resistivity value of 3.38 Ωm at depths from 19.30 – 23.04 meters, is interpreted as a mixture of clay and sand. The fifth layer, ranging from a depth of 23.04 – 41.28 meters, shows a resistivity value of 222.44 Ωm and is identified as a layer of sandy clay and gravel. The sixth layer, at depths from 41.28 – 49.32 meters, shows a resistivity value of 498.00 Ωm and is interpreted as dry sand and gravel. The last layer, at depths from 49.32 – 60.00 meters, has a resistivity value of 1300.53 Ωm and is identified as dry sand and gravel. The interpretation results of track 1 data can be seen in Table 3.

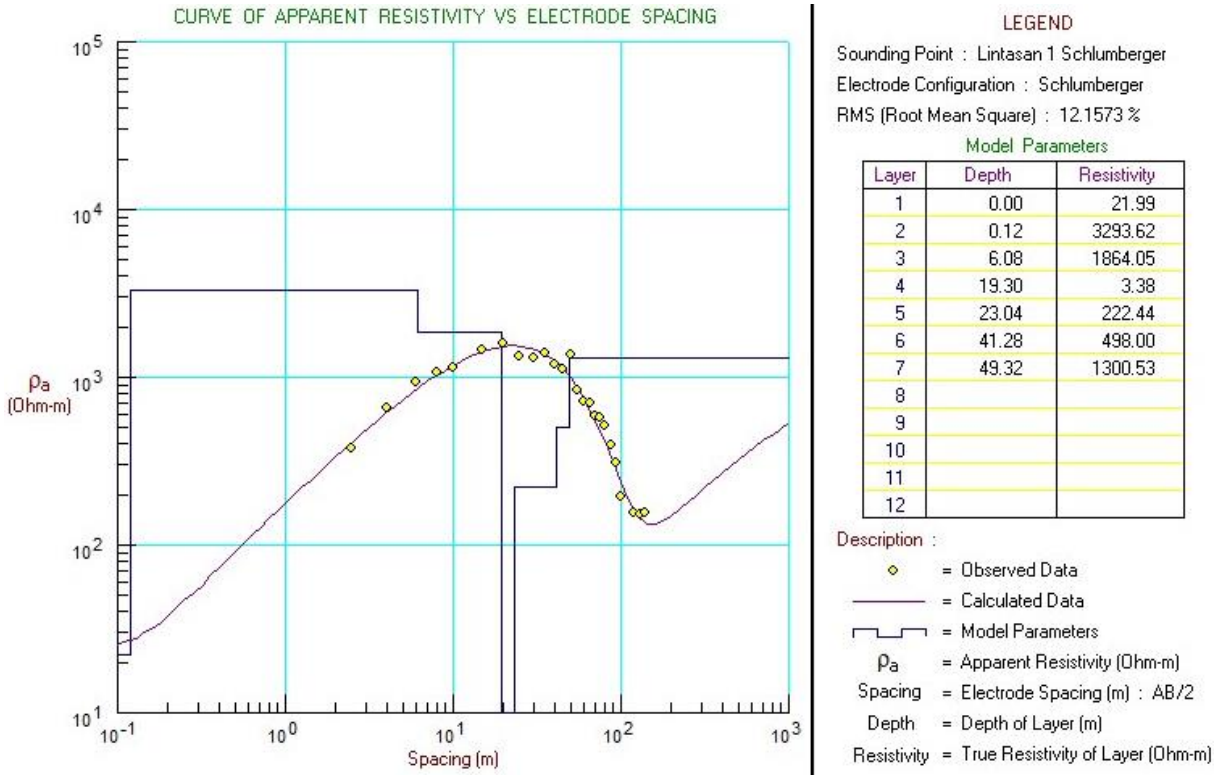

Figure 4. Progress interface of vertical model data processing - track 1.

Table 3. Description of interpretation results for track 1 Schlumberger configuration.

Resistivity (Ωm)	Depth (m)	Distance (m)	Rock type	Information
21.99	0.00 – 0.12	0.12	Sand and clay	Non aquifer
3,293.62	0.12 – 6.08	5.96	Sandstone and limestone	Aquifer
1,864.05	6.08 – 19.30	13.22	Dry sand and gravel	Aquifer
3.38	19.30 – 23.04	3.74	Clay and sand	Non aquifer
222.44	23.04 – 41.28	18.24	Sand clay and gravel	Non aquifer
498.00	41.28 – 49.32	8.04	Sand and gravel	Aquifer
1,300.53	49.32 – 60.00	10.68	Dry sand and gravel	Aquifer

3.4. Interpretation of Vertical Geoelectric Data Model – Track 2

Track 2 is located at coordinate 0°25'10.0"N 101°19'46.9"E, running from North to South. The modeling results of track 2 using the vertical model are clearly depicted in Figure 5 using the Progress software. From the model, the resistivity interval on this track ranges from 12.02 – 1,478.31 Ωm, with 7 layers identified through resistivity values and depths from the ground surface.

The model shown in Figure 5 represents the progress interface presenting resistivity values along with the depth of each layer. It is evident that on track 2, using the vertical model, the layer depth is 47.04 meters with an RMS-error value of 10.16%. The interpretation results of track 2 data can be seen in Table 4.

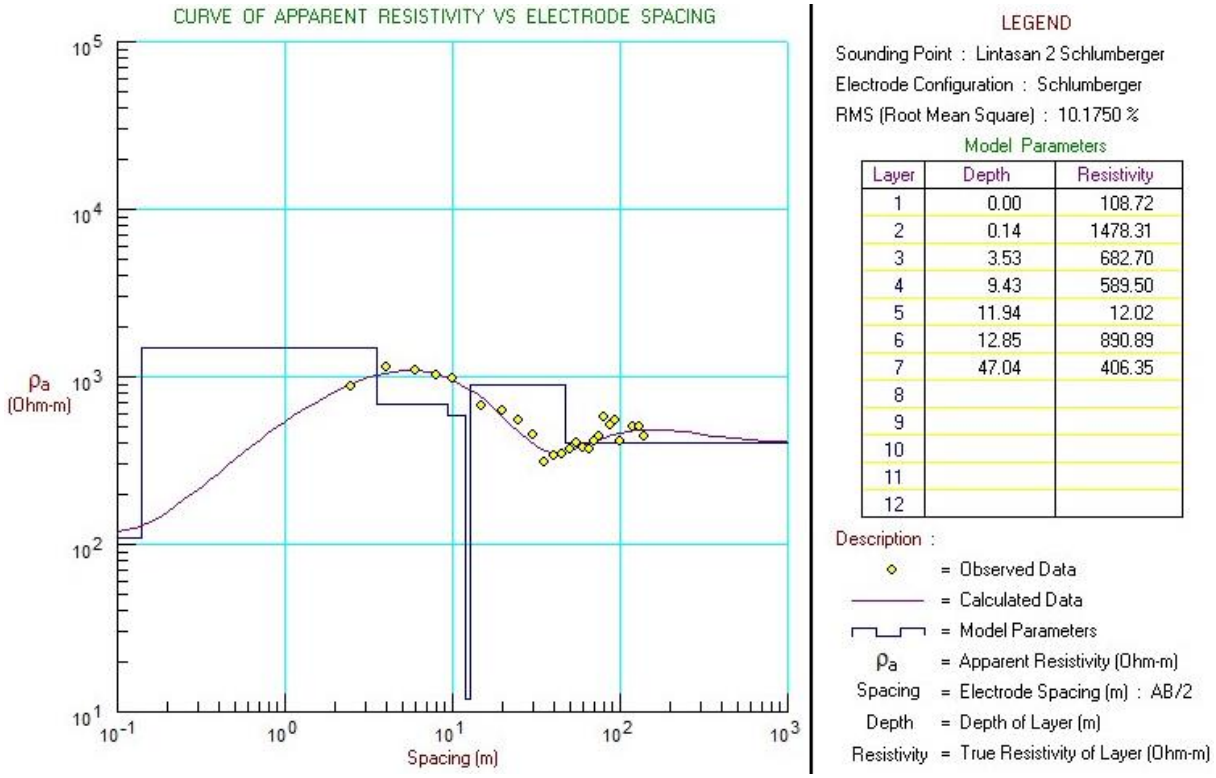

Figure 5. Progress interface of vertical model data processing - track 2.

Table 4. Description of interpretation results for track 2 Schlumberger configuration.

Resistivity (Ωm)	Depth (m)	Distance (m)	Rock type	Information
108.72	0.00 – 0.14	0.14	Sand clay and gravel	Non aquifer
1478.31	0.14 – 3.53	3.39	Dry sand and gravel	Aquifer
682.70	3.53 – 9.43	5.9	Dry sand and gravel	Aquifer
589.50	9.43 – 11.94	2.51	Sandstone	Aquifer
12.02	11.94 – 12.85	0.91	Sand and clay	Non aquifer
890.89	12.85 – 47.04	34.19	Dry sand and gravel	Aquifer
12.96	47.04 – 60.00	12.96	Dry sand and gravel	Aquifer

The underground layers with resistivity value of 108.72 Ωm at depths from 0.00 – 0.14 meters are interpreted as a mixture of sandy clay and gravel, while the second layer, with depths ranging from 0.14 – 3.53 meters and a resistivity value of 1478.31 Ωm, is identified as dry sand and gravel. The third layer, with depths from 3.53 – 9.43 meters and a resistivity value around 682.70 Ωm, is interpreted as a layer of dry sand and gravel. Furthermore, the fourth layer with a resistivity value of 589.50 Ωm and depths from approximately 9.43 – 11.94 meters is interpreted as sandstone. The fifth layer, at depths from 11.94 to 12.85 meters, is identified as a mixture of sand and clay with a resistivity value of 12.02 Ωm. The sixth layer has a resistivity value ranging from 890.89 Ωm at

depths from 12.85 – 47.04 meters, interpreted as dry sand and gravel. The last layer, at depths from 47.04 – 60.00 meters, is identified as dry sand and gravel with a resistivity value of 406.35 Ωm.

3.5. Discussion of Geoelectric Data Results

3.5.1. Horizontal Geoelectric Model Data

The geoelectric measurements using the horizontal model reveal that each research track consists of multiple rock layers with varying resistivity and different depths. The resistivity values of rocks are influenced by factors such as water content, porosity, density, and permeability of the rock layers. Rock layers with high resistivity act as aquifers with low productivity due to the dry conditions of the layers, while rock layers with low resistivity have the potential to be aquifers with high productivity [22]. Data from track 1, with layers having resistivity values ranging from 26.7 – 100 Ωm, are interpreted as non-aquifer layers dominated by clay, indicating the presence of a semi-permeable basal layer (aquitard) containing groundwater. Meanwhile, the layers at depths of 2.50 – 24.9 meters with resistivity values of 100 – 378 Ωm are dominated by gravel and some clay, classifying them as water-bearing layers (aquifers). Sandstone typically has a normal porosity density ranging from 10% – 20%, allowing it to store groundwater and facilitate water flow. Layers with resistivity values of 378 – 5,343 Ωm are interpreted as effective aquifer layers, consisting of gravel and sandstone with a combination of high porosity and good permeability. Furthermore, layers with resistivity values of 5,343 – 20,102 Ωm are identified as limestone, which is an aquifer layer with high porosity, primarily due to the presence of calcite (calcium carbonate) that dissolves. When water infiltrates limestone, calcite dissolution can occur, leaving pores in the rock that allow water to accumulate. Limestone structures generally serve as significant groundwater sources and can be utilized for drinking water supply. Additionally, karstification in limestone rocks can create complex and fascinating groundwater systems. The last layer consisting of quartzite with resistivity ranging from 75,628 – 28,4524 Ωm is not considered an aquifer layer. This is due to the low porosity and permeability of quartzite, resulting from its dense grain structure and lack of natural water channels within the rock. Therefore, water cannot easily flow through quartzite, making it ineffective as an aquifer layer.

Data from track 2, with resistivity intervals of 1.49 – 33.1 Ωm, are interpreted as layers containing clay and sand, forming a semi-impermeable layer that allows water to flow, albeit slowly. The layers found at depths from 2.5 – 24.9 meters with resistivity values of 156 – 736 Ωm are identified as alluvium. Alluvium generally consists of a mixture of sand, gravel, mud, and other deposit obtained through deposition processes by water flow and has relatively high porosity ranging from 20% – 40%, making it an effective aquifer. Furthermore, layers with resistivity values of 736 – 16,348 Ωm constitute aquifer layers consisting of limestone. Limestone is known to have a good porosity level ranging from 5% – 30%, allowing it to efficiently transmit water. The last layer, with resistivity values ranging from 7,706 – 16,348 Ωm, is interpreted as a non-aquifer layer because it contains quartzite. Quartzite, with its dense grain structure and low permeability, cannot effectively transmit water through the rock matrix.

3.5.2. Vertical Geoelectric Model Data

Geoelectric resistivity measurements using the Schlumberger configuration rule show data processing results using the Progress software, which can be seen in Figure 4 and Figure 5. Aquifer layers obtained from the data processing results on track 1 and track 2 indicate the distribution of groundwater. Aquifer layers containing groundwater are found at depths of 6.08 – 19.30 meters and 3.53 – 9.43 meters. The resistivity values shown in Figures 4 and 5 indicate that areas with soil and subsurface rock layers with intervals ranging from 406.35 – 3,293.62 Ωm can be interpreted as permeable layers. These layers consist of gravel and sand. They allow groundwater to flow because sand and gravel have large porosity, making these layers potentially capable of transmitting and storing groundwater [23, 24]. These findings are significant, consistent with interviews with local residents indicating that well depths in the area typically range from around 7 – 15 meters.

Peat layers contain fluid because they have the ability to absorb water. A layer with resistivity of 589.50 Ωm can be interpreted as a sandstone layer. This layer allows for the presence of groundwater, although the amount is not significant. The potential groundwater storage in rocks

depends on the permeability of the rock [25-27]. Groundwater flow in this study tends to be dispersed and occurs at certain depths, as seen in the obtained resistivity values. Groundwater distribution in the research area extends 100 meters from East to West and from North to South.

The cover layer is the topmost layer, interpreted in this research area as fill soil with a thickness of approximately 1 meter. The conductive zone, with resistivity values less than 1000 Ωm, is referred to as the unsaturated aquifer zone. The resistive layer, with resistivity intervals greater than 1000 Ωm, is relatively lower and is presumed to be the basement. The resistivity interval of the cover layer is quite long and is dominated by conductive layers [28, 29]. Layers with resistivity values ranging from 200 – 1000 Ωm are presumed to be layers with denser porosity but can be filled with water, also known as aquitard, with lithological components believed to be sand, limestone, and dry gravel. Layers with resistivity values greater than 1000 Ωm are interpreted as layers dominated by impermeable rock [30, 31]. The lithology in this research area is not exactly the same as the lithology map of the Tambang District because its surface has been filled for housing development.

4. CONCLUSION

In summary, based on the resistivity measurement results, interpretation of the horizontal model indicates that traverse 1 exhibit a range of soil layer resistivity between 26.7 Ωm and 284524 Ωm, with a maximum depth of 24.9 meters. Meanwhile, traverse 2 shows soil resistivity values ranging from 1.49 – 7706 Ωm. Interpretation results using the vertical model show that traverse 1 has resistivity ranging from 3.38 – 3293.62 Ωm, with a maximum depth of 49.32 meters. Traverse 2 exhibits a soil resistivity range between 12.02 Ωm and 1478.31 Ωm, with a depth of up to 47.04 meters. The presence of aquifers is confirmed based on the formation of geological map sheets, data processing, and 2D geoelectric cross-sectional images of the horizontal model. Interpretation of traverse 1 reveals aquifer depths at 6.50 meters and 19 meters, consisting of gravel, sandstone, and limestone lithology. On traverse 2, aquifers are found at depths ranging from 2.50 – 24.9 meters, with lithology composed of alluvium, gravel, and limestone. Interpretation results from the 1D geoelectric vertical model cross-section show that traverse 1 is found at depths of 0.12 meters, 19.30 meters, and beyond 41.28 meters, with lithology consisting of sandstone, limestone, and dry gravel. Meanwhile, traverse 2 is found at depths of 0.14 meters, 9.43 meters, and beyond 12.02 meters, with lithology composed of sand and dry gravel.

REFERENCES

[1] Negassa, W., Acksel, A., Eckhardt, K. U., Regier, T., & Leinweber, P. (2019). Soil organic matter characteristics in drained and rewetted peatlands of northern Germany: Chemical and spectroscopic analyses. *Geoderma*, **353**, 468–481.

[2] Osaki, M., Kato, T., Kohyama, T., Takahashi, H., Haraguchi, A., Yabe, K., Tsuji, N., Shiodera, S., Rahajoe, J. S., Atikah, T. D., Oide, A., Matsui, K., Wetadewi, R. I., & Silsigia, S. (2021). Basic information about tropical peatland ecosystems. *Tropical Peatland Eco-Management*, 3–62.

[3] Mulyani, I. (2020). Potensi dan tantangan pemberdayaan masyarakat lahan gambut: Studi pendekatan kehidupan berkelanjutan di Kelurahan Tanjung Palas Kecamatan Dumai Timur Kota Dumai. *KOMUNITAS*, **11**(1), 1–20.

[4] Ehara, H., Kakuda, K., Miyazaki, A., Naito, H., Nakamura, S., Nitta, Y., Okazaki, M., Sasaki, Y., Toyota, K., Watanabe, A., Watanabe, M., Yamamoto, Y., Goto, Y., & Kimura, S. D. (2021). Sago palm in peatland. *Tropical Peatland Eco-Management*, 477–507.

[5] Ardiyani, V. (2022). *The impact of 2018/2019 wildfire exposure on BaP-DNA adducts and birth weight in Indonesia*. Doctoral dissertation, King's College London.

[6] Riono, Y. & Apriyanto, M. (2020). Pemanfaatan abu sekam padi dalam inovasi pemupukan kacang hijau (Vigna Radiate L) di lahan gambut. *Selodang Mayang: Jurnal Ilmiah Badan Perencanaan Pembangunan Daerah Kabupaten Indragiri Hilir*, **6**(2), 60.

[7] Williamson, J., Evans, C., Spears, B., Pickard, A., Chapman, P. J., Feuchtmayr, H., ... & Monteith, D. (2020). Will UK peatland restoration reduce dissolved organic matter concentrations in upland drinking water supplies?. *Hydrology and Earth System Sciences Discussions*, **2020**, 1–21.

[8] Soewandita, H. (2018). Kajian pengelolaan tata air dan produktivitas sawit di lahan gambut (Studi kasus: lahan gambut perkebunan sawit PT Jalin Vaneo di Kabupaten Kayong Utara, Propinsi Kalimantan Barat). *Jurnal Sains dan Teknologi Modifikasi Cuaca*, **19**(1), 41–50.
[9] Juandi, M. & Santoso, S. A. (2021). Analysis of groundwater infiltration using the schlumberger geoelectric method. *Journal of Physics: Conference Series*, **2049**(1), 012070.
[10] Kumar, V., Singh, E., Singh, S., Pandey, A., & Bhargava, P. C. (2023). Micro-and nano-plastics (MNPs) as emerging pollutant in ground water: Environmental impact, potential risks, limitations and way forward towards sustainable management. *Chemical Engineering Journal*, **459**, 141568.
[11] Hojjati-Najafabadi, A., Mansoorianfar, M., Liang, T., Shahin, K., & Karimi-Maleh, H. (2022). A review on magnetic sensors for monitoring of hazardous pollutants in water resources. *Science of The Total Environment*, **824**, 153844.
[12] Sutasoma, M., Azhari, A. P., & Arisalwadi, M. (2018). Identifikasi air tanah dengan metode geolistrik resistivitas konfigurasi Schlumberger di Candi Dasa Provinsi Bali. *Konstan-Jurnal Fisika Dan Pendidikan Fisika*, **3**(2), 58–65.
[13] Sambo, C., Dudun, A., Samuel, S. A., Esenenjor, P., Muhammed, N. S., & Haq, B. (2022). A review on worldwide underground hydrogen storage operating and potential fields. *International Journal of Hydrogen Energy*, **47**(54), 22840–22880.
[14] Juandi, M. (2018). The interpretation of underground water physical parameters of housing in the region of asahan indah palm oil factory area Rokan Hulu District. *Open Journal of Modern Hydrology*, **8**(4), 119–125.
[15] Sendrós, A., Urruela, A., Himi, M., Alonso, C., Lovera, R., Tapias, J. C., Rivero, L., Garcia-Artigas, R., & Casas, A. (2021). Characterization of a shallow coastal aquifer in the framework of a subsurface storage and soil aquifer treatment project using electrical resistivity tomography (Port de la Selva, Spain). *Applied Sciences*, **11**(6), 2448.
[16] González, J. A. M., Comte, J. C., Legchenko, A., Ofterdinger, U., & Healy, D. (2021). Quantification of groundwater storage heterogeneity in weathered/fractured basement rock aquifers using electrical resistivity tomography: Sensitivity and uncertainty associated with petrophysical modelling. *Journal of Hydrology*, **593**, 125637.
[17] Sohibun, S. (2019). Aplikasi metode geolistrik konfigurasi schlumberger untuk mengidentifikasi lapisan air tanah di Desa Ulak Patian Rokan Hulu Riau. *Jurnal Fisika Flux: Jurnal Ilmiah Fisika FMIPA Universitas Lambung Mangkurat*, **16**(1), 54–60.
[18] Kumar, D., Mondal, S., & Warsi, T. (2020). Deep insight to the complex aquifer and its characteristics from high resolution electrical resistivity tomography and borehole studies for groundwater exploration and development. *Journal of Earth System Science*, **129**(1), 68.
[19] Abudeif, A. M., Mohammed, M. A., Fat-Helbary, R. E., El-Khashab, H. M., & Masoud, M. M. (2020). Integration of 2D geoelectrical resistivity imaging and boreholes as rapid tools for geotechnical characterization of construction sites: a case study of New Akhmim city, Sohag, Egypt. *Journal of African Earth Sciences*, **163**, 103734.
[20] Choudhury, K., Saha, D. K., & Chakraborty, P. (2001). Geophysical study for saline water intrusion in a coastal alluvial terrain. *Journal of applied geophysics*, **46**(3), 189–200.
[21] Ray, L. K. J. R. (1989). *Hidrologi untuk Insinyur 3ed*. Jakarta: Erlangga.
[22] Buwana, B., Priyantari, N., & Supriyadi, S. (2020). Identification of aquifer in the MIPA Faculty-University of Jember using 1D geoelectrical resistivity method with Schlumberger array. *Jurnal ILMU DASAR*, **21**(2), 123–132.
[23] Manrulu, R. H., Nurfalaq, A., & Hamid, I. D. (2018). Pendugaan sebaran air tanah menggunakan metode geolistrik resistivitas konfigurasi wenner dan schlumberger di kampus 2 universitas cokroaminoto palopo. *Jurnal Fisika Flux: Jurnal Ilmiah Fisika FMIPA Universitas Lambung Mangkurat*, **15**(1), 6–12.
[24] Malik, U., Defrianto, D., Zulfa, Z., Saputra, Y. D., & Muhammad, J. (2023). One-dimensional analysis of underground water using geoelectric methods. *Science, Technology and Communication Journal*, **4**(1), 11–14.
[25] Hanifa, D., Sota, I., & Siregar, S. S. (2016). Penentuan lapisan akuifer air tanah dengan metode geolistrik konfigurasi chlumberger di desa Sungai Jati Kecamatan Mataraman Kabupaten Banjar

Kalimantan Selatan. *Jurnal Fisika Flux: Jurnal Ilmiah Fisika FMIPA Universitas Lambung Mangkurat*, **13**(1), 30–39.

[26] Zulkarnain, Z., Kurniawati, R., Triwulandari, T., Husein, I. R., & Kurniawan, R. (2023). Water seepage rate in composted soil. *Science, Technology and Communication Journal*, **3**(3), 95–100.

[27] Adjisetya, M., Wahid, A., & Rohman, I. A. (2023). Modelling and control of nonlinear compressor unit in biohydrogen plant using multivariable model predictive control (MMPC). *Science, Technology and Communication Journal*, **3**(3), 63–70.

[28] Telford, W. M. (1990). *Applied Geophysics 2nd*. Cambridge: Cambridge University Press.

[29] Nurhedi, P. R. & Muhammad, J. (2023). Analisis penurunan kadar air gaplek menggunakan alat pengering kabinet berbasis biomassa tempurung kelapa. *Indonesian Physics Communication*, **20**(2), 123–126.

[30] Sarmauli, O., Setyawan, A., & Dwiyanto, J. S. (2016). Identifikasi potensi akuifer berdasarkan metode geolistrik tahanan jenis pada daerah krisis air bersih di Kota Semarang. *Youngster Physics Journal*, **5**(4), 327–334.

[31] Handayani, M. & Muhammad, J. (2022). Aplikasi uji coba skala laboratorium implementasi prototype alat inovasi teknologi pasca panen berbasis biomassa untuk deteksi temperature dengan sistem internet of things. *Indonesian Physics Communication*, **19**(2), 69–74.